

# Identification of sulfate sources in groundwater using isotope analysis and modeling of flood irrigation with waters of different quality in the Jinghuiqu district of China

Xiuhua Liu · Jirka Šimůnek · Lin Li ·  
Junqi He

Received: 9 February 2012 / Accepted: 12 September 2012 / Published online: 25 September 2012  
© Springer-Verlag Berlin Heidelberg 2012

**Abstract** The main objective of this study was to identify the main sources and processes that control  $\text{SO}_4^{2-}$  groundwater concentrations in the Jinghuiqu irrigation district of China using isotope analysis. Lysimeter irrigation experiments and numerical modeling were used to assess the impact of long-term irrigation practices on sulfate transport, when different sources of irrigation water were used.  $\text{SO}_4^{2-}$  concentrations in the groundwater of the entire irrigation area increased significantly from the years 1990 (a mean value was  $4.8 \text{ mmol L}^{-1}$ ) to 2009 (a mean value was  $9.84 \text{ mmol L}^{-1}$ ). The  $\delta^{34}\text{S-SO}_4^{2-}$  values (ranging from  $+5.27$  to  $+10.69$  ‰) indicated that sulfates in groundwater were initially predominantly derived from dissolution of minerals. However, no soluble sulfate minerals (gypsum and/or mirabilite) were detected after 1990. To better understand this seeming anomaly, water content and  $\text{SO}_4^{2-}$  data were collected before and after the field irrigation experiment and analyzed using the HYDRUS-1D and HP1 software packages. The experimental data were

also used to assess sulfate leaching when different sources of irrigation water were used under current irrigation practices. The dissolved sulfate concentrations in the soil profile increased significantly when groundwater was used for infiltration compared to the use of surface water. Irrigation water sources had a great impact on the increase of sulfate concentrations in the shallow groundwater, especially when groundwater with elevated concentrations was used for irrigation.

**Keywords** Sulfate · Stable isotopes · Irrigation · Transport and leaching · HYDRUS-1D and HP1 models

## Introduction

Groundwater pollution is increasingly a concern in many irrigated areas with arid, semi-arid, and even sub-humid climates with persistently scarce rainfall conditions. Jinghuiqu ( $34^\circ 25' 20''$ – $34^\circ 41' 40''\text{N}$ ,  $108^\circ 34' 34''$ – $109^\circ 21' 35''\text{E}$ ) is a large irrigation district located in the middle of the Guanzhong plain of the Shaanxi Province of China (Fig. 1). The total area of this irrigation district is  $1,180 \text{ km}^2$ . It belongs to the catchment of the Weihe River, a Cenozoic fault-block basin filled predominantly with Tertiary fluvial and aeolian sediments and Quaternary loess (Bellier et al. 1988). The upper part of the sedimentary filling consists mainly of Quaternary fluvial deposits (Fig. 2), having mostly a sandy clay loam texture. The district has experienced 2,200 years of irrigation history, and currently possesses a high population density (Liu and Zhu 2011).

Due to being located in the semi-arid region, the Jinghuiqu district has a shortage of water resources for irrigation. So far, existing research has focused mainly on

---

X. Liu (✉)  
Department of Environmental Science and Engineering,  
Chang'an University, No.126 Nanduan Yanta Road,  
Xi'an 710054, China  
e-mail: liuxh68@chd.edu.cn

J. Šimůnek  
Department of Environmental Sciences, University of California  
Riverside, Riverside, CA 92521, USA

L. Li  
Xi'an Center of Geological Survey, China Geological Survey,  
Xi'an 710054, China

J. He  
Water and Development Institute, Chang'an University,  
Xi'an 710054, China

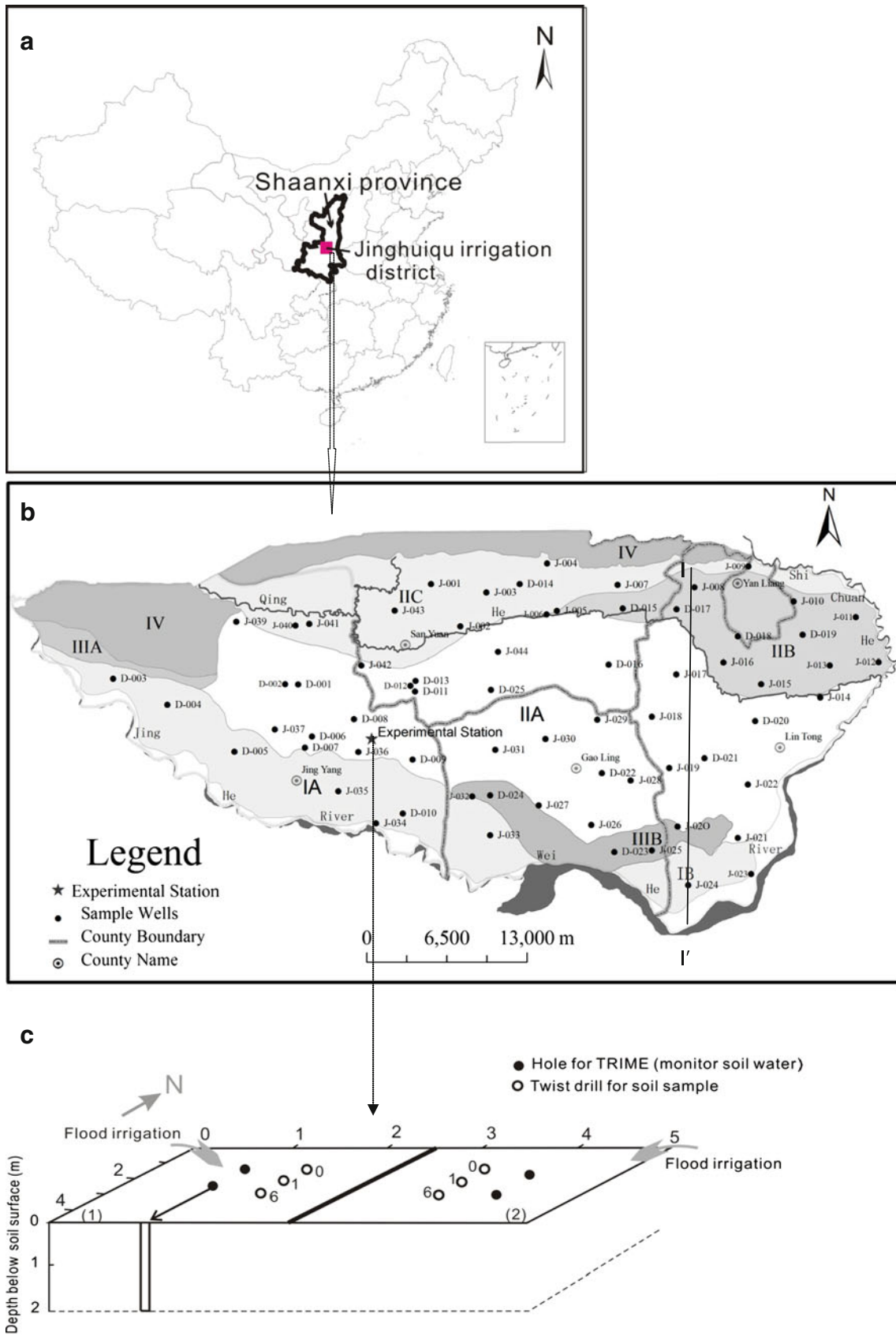


**Fig. 1 a** A map showing the location of the irrigation district in China. **b** A map of the Jinghuiqu irrigation district (the Shaanxi province, China) and the location of groundwater sampling wells. *Different colors and symbols* (e.g., IA, IIA) represent hydrogeological conditions: IA—the Jinghe river first terrace strong water-rich sub-district, IIA—the Jinghe river second terrace water-rich sub-district (south of the Yeyuhe and Qihe rivers), IIIA—the Jinghe river third terrace water-rich sub-district, IB—the Weihe river first terrace strong water-rich sub-district, IIB—the Jinghe river second terrace water-rich sub-district (north of the Qihe river), IIIB—the Weihe river second terrace water-rich sub-district, IIC—the Jinghe river second terrace water-rich sub-district (north of the Yeyuhe and Qihe rivers), IV—the Loess Plateau weak water-rich sub-district. **c** The experimental arrangement. *x, y, and z axes are in meters. Plot (1) was irrigated only with groundwater, while plot (2) was irrigated with groundwater and the fertilizer ((NH<sub>4</sub>)<sub>2</sub>HPO<sub>4</sub>). The numbers 0, 1, and 6 in the plots indicate times of the sampling (at the beginning of the experiment, and 1 and 6 days after irrigation) using a twist drill*

quantitative water-related issues, such as irrigation systems (Li 1998; Liu 2002), irrigation techniques (Gao 2004), optimization of water use, the efficient use of irrigation water, and an optimal conjunctive use of surface and groundwater (Liu 2005; Zhao and Fei 2006; Li et al. 1999; Liu and Zhu 2011). Since 1990, due to the lack of available surface water, the Jinghuiqu district has increased pumping from the aquifers to provide water for irrigation, which has resulted in a significant drop in the groundwater table (Liu 2010). However, research is still lacking on qualitative water-related issues, such as the evolution of sulfate concentrations in the groundwater.

The field survey in the Jinghuiqu district showed that the groundwater had become seriously polluted with SO<sub>4</sub><sup>2-</sup>, which is a very important and widespread environmental problem in many irrigated agricultural regions (Böhlke 2002; Rock and Mayer 2009; Szykiewicz et al. 2011). Models evaluating these environmental risks should consider an integrated approach (Ramos et al. 2011), and should be capable of predicting water and solute movement in the vadose zone and analyzing specific laboratory or field experiments involving unsaturated water flow and

solute transport (Gonçalves et al. 2006). Such models could provide helpful tools for extrapolating information from a limited number of field experiments to different soil types, crops, and climatic conditions, as well as to different tillage and water irrigation management schemes (Gonçalves et al. 2006; Forkutsa et al. 2009; Ramos et al. 2011).

The first objective of this study was to identify historical SO<sub>4</sub><sup>2-</sup> sources and controlling hydrogeochemical processes in the groundwater using stable isotopes and by analyzing spatial and temporal variations of SO<sub>4</sub><sup>2-</sup> in the groundwater of the entire irrigation area. The second objective was to use the lysimeter irrigation experiment to assess sulfate leaching when different irrigation water sources were used under current irrigation conditions, and to show the impact of long-term irrigation on sulfate evolution in the groundwater in the Jinghuiqu irrigation district. While the former objective was addressed by analyzing temporal changes of SO<sub>4</sub><sup>2-</sup>, the latter objective was achieved by evaluating lysimeter data using the HYDRUS-1D and HP1 software packages. The lysimeter experiment was intended to replicate current irrigation methods and conditions to determine whether the elevated SO<sub>4</sub><sup>2-</sup> in the groundwater is controlled by the different irrigation water sources or the sulfate minerals in deposits.

**Materials and methods**

**Irrigation district**

In the Jinghuiqu irrigation district, both surface water (from the Jinghe River) and groundwater are used by farmers for surface flood irrigation. The climate is semiarid and has a mean annual precipitation of about 533 mm, with nearly 60 % of the annual rainfall received between July and September. The mean annual temperature is 13.6 °C, with a maximum of 42 °C in July and a minimum of -24 °C in

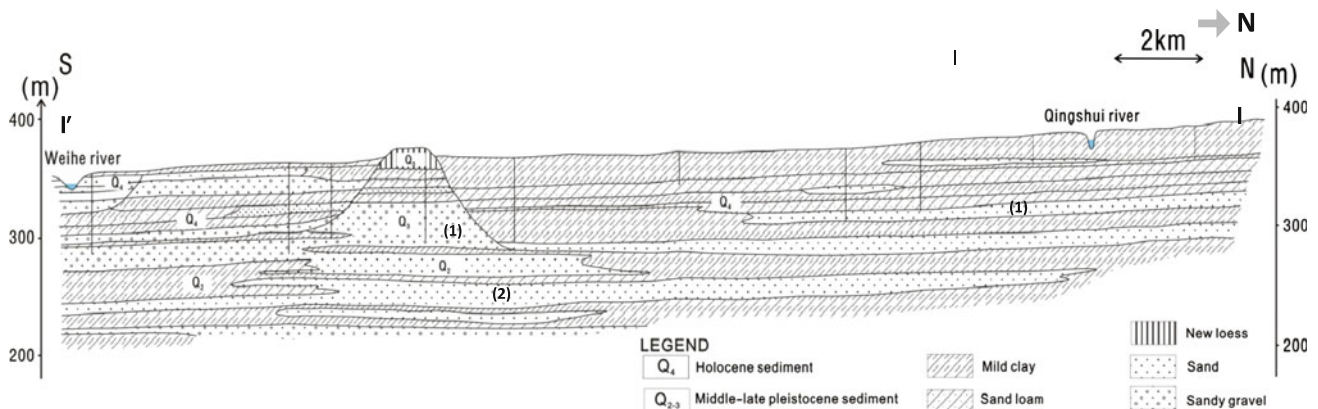


**Fig. 2** Cross-section of the Jinghuiqu irrigation district and locations and depths of sampling wells (from the Groundwater Investigation Report of Jinghuiqu, Jinghuiqu Irrigation District 1983; (1) unconfined aquifer; (2) confined aquifer)

**Table 1** Ionic compositions of waters used in the irrigation experiment (mmol L<sup>-1</sup>)

Water type	HCO <sub>3</sub> <sup>-</sup>	Cl <sup>-</sup>	SO <sub>4</sub> <sup>2-</sup>	Ca <sup>2+</sup>	Mg <sup>2+</sup>	Na <sup>+</sup>	pH
Surface water <sup>a</sup>	5.21	3.16	2.45	1.45	1.8	7.1	8.02
Groundwater (1) <sup>b</sup>	5.30	3.50	1.51	0.72	0.41	3.02	7.82
Groundwater (2) <sup>c</sup>	10.9	8.59	9.64	1.81	6.55	21.0	7.59

<sup>a</sup> Used in the irrigation experiment in November of 2009

<sup>b</sup> Used in the irrigation experiment in November of 2008

<sup>c</sup> Mean values for irrigation district groundwater in November of 2009

January. The average annual potential evapotranspiration is 1,212 mm. While winter wheat and maize are generally irrigated using water from the aquifer between June and September, surface water is typically used between November and May to preserve the ground water table. Typically, the fields of the irrigation district are irrigated 3–5 times a year, depending on the amount of precipitation. The quantity of water used for flood irrigation ranges from 18 to 24 cm.

#### Groundwater sampling

Groundwater samples were collected in April 1990 (from 91 wells), November 2008 (46 wells), and December 2009 (46 wells) in the Jinghuiqu irrigation district for chemical and isotopic analyses (2008) from both shallow and deep (more than 50 m below the surface) wells used for domestic and agricultural water supply. Sampling locations are shown in Fig. 1b. The same sampling locations were used in different years. As groundwater levels dropped after 1990, several well screens were above the groundwater table in 2008/2009 and could not be used for the second sampling round. Groundwater samples were collected directly from the wells with the submersible pump. The groundwater samples, collected over a 3-day period, were filtered through a 0.45-mm membrane, and stored in 60 mL polyethylene bottles for chemical analysis.

#### Field experiments

Field infiltration processes were studied in the soil profile irrigated with groundwater at the experimental station of the Jinghuiqu irrigation area (Fig. 1c). Two experimental sites (with a size of 11 m<sup>2</sup> × 2.0 m deep each) were constructed for this purpose. To prevent lateral movement of surface irrigation water, the sites were laterally isolated with mounds. They were then exposed to atmospheric conditions. The sites were bare (not covered by vegetation) during the experiments. They were manually surface flood irrigated with 18 cm (nearly 2 m<sup>3</sup>) of groundwater during the normal irrigation period in November 2008. Irrigation water used for experimental irrigation was collected on

November 11, 2008, and monitored for concentrations of Na<sup>+</sup>, Ca<sup>2+</sup>, Mg<sup>2+</sup>, SO<sub>4</sub><sup>2-</sup>, HCO<sub>3</sub><sup>-</sup>, and Cl<sup>-</sup> (Table 1, groundwater (1)).

At the beginning of the experiment, and at 1 and 6 days after irrigation, soil samples were collected using the twist drill from 6 depths of 0–20, 20–40, 40–60, 60–100, 100–150, and 150–200 cm (mixed samples were used, e.g., the 0- to 20-cm soil sample was mixed from soil collected between depths of 0 and 20 cm). Samples were stored in a dark chamber and kept at 4 °C until laboratory measurements the next day. Ion concentrations of Cl<sup>-</sup>, SO<sub>4</sub><sup>2-</sup>, HCO<sub>3</sub><sup>-</sup>, Na<sup>+</sup>, K<sup>+</sup>, Ca<sup>2+</sup>, and Mg<sup>2+</sup> in the soil samples were measured by diluting the soil solution in water (1:5 soil/solution) and allowing it to interact for 3 min with the solution. All measurements were performed using three replicates.

The soil water contents were measured during the irrigation experiment using the TDR (Time Domain Reflectometry) system (Intelligent Micromodule Elements, TRIME, IMKO, Germany) before irrigation, and at 1 and 5 days after irrigation, at 20-cm intervals between depths of 0.2 and 2 m. The TRIME portable borehole packer unit used here has a two-electrode probe configuration, with 150-mm long electrodes made from lead. The manufacturer indicates that the measurement error of the borehole packer is about ±0.2 %. The packer is lowered into a 100-mm diameter, uncased borehole and then inflated to push the electrodes close to the borehole wall, according to the method described by West and Truss (2006). The borehole was cased to a 2-m depth with a PE pipe to prevent its collapse. Three readings were taken at each depth and averaged. The manufacturer's calibration was used, which converts the measured travel time of a signal directly into the water content of the material in contact with the packer. The measured water contents ( $\theta$ ) and their statistics are presented in Table 2.

#### Sample analyses

The pH was measured using a potentiometric method. Samples for cation analysis were preserved using ultra-pure HNO<sub>3</sub>. Cations were analyzed using inductively coupled plasma-atomic emission spectrometry (ICP-AES). Anions

**Table 2** Measured water contents and corresponding statistics during the irrigation experiment (cm<sup>3</sup> cm<sup>-3</sup>)

Time (days)	Number of samples	Maximum	Minimum	Mean	Standard deviation	Coefficient of variation (%)
0	9	0.28	0.18	0.22	0.03	0.14
1	9	0.41	0.22	0.3	0.06	0.20
2	9	0.35	0.23	0.29	0.04	0.14
3	9	0.34	0.23	0.28	0.03	0.11
4	9	0.32	0.25	0.28	0.03	0.11

**Table 3** Measured SO<sub>4</sub><sup>2-</sup> and Cl<sup>-</sup> concentrations in groundwater and corresponding statistics in 1990, 2008, 2009, and 2011 (mmol L<sup>-1</sup>)

Variable	Number of samples	Maximum	Minimum	Mean	Standard deviation	Coefficient of variation (%)	Frequency distributions of more than 250 mg L <sup>-1</sup> (%)	Frequency distributions of more than 600 mg L <sup>-1</sup> (%)
1990								
Cl <sup>-</sup>	90	38.0	2.63	7.8	4.36	0.59	49.4	
SO <sub>4</sub> <sup>2-</sup>	90	16.5	1.5	4.8	2.29	0.48	92	16.5
2008								
Cl <sup>-</sup>	46	31.5	2.25	8.48	5.02	0.59	52.2	
SO <sub>4</sub> <sup>2-</sup>	46	23.5	2.0	9.23	4.41	0.76	97.8	73.9
δ <sup>34</sup> S (‰)	11	10.7	5.27	9.11	1.5	0.16		
2009								
Cl <sup>-</sup>	46	24.2	1	8.59	4.38	0.51	61.7	
SO <sub>4</sub> <sup>2-</sup>	46	21.9	1.55	9.84	4.37	0.44	97.8	85.1
2011								
Cl <sup>-</sup>	41	17.7	1.5	8.65	3.23	0.37	69.6	
SO <sub>4</sub> <sup>2-</sup>	41	35.0	2.63	13.7	5.18	0.38	100	95.1

δ<sup>34</sup>S is also given for 2009

Cl<sup>-</sup> and SO<sub>4</sub><sup>2-</sup> were measured with ion chromatography. Bicarbonate (HCO<sub>3</sub><sup>-</sup>) was measured by acid–base titration. Cation and anion concentrations were determined with a detection limit of 0.001 mmol/L and an accuracy better than 2 %. Table 3 presents the statistics for groundwater Cl<sup>-</sup> and SO<sub>4</sub><sup>2-</sup> concentrations in 1990, 2008, 2009, and 2011.

Eleven groundwater samples from 2008 were selected for the analysis of δ<sup>34</sup>S values of SO<sub>4</sub><sup>2-</sup>, assuming uniform distribution in each hydrogeological unit. Sulfates in groundwater were precipitated as BaSO<sub>4</sub>, and δ<sup>34</sup>S values were determined in the State Key Laboratory of Environmental Geochemistry at the Institute of Geochemistry Guiyang, as described by Shanley et al. (2005). Stable isotope ratios were reported in the usual δ notation, with respect to international standards V-CDT (Vienna Canyon Diablo Troilite) for sulfur isotope measurements. An average precision of measurements was ±0.3 ‰ for δ<sup>34</sup>S-SO<sub>4</sub><sup>2-</sup> values. The measured δ<sup>34</sup>S-SO<sub>4</sub><sup>2-</sup> and their statistics are presented in Table 3.

The isotopic composition of sulfate has been successfully used for examining sources and pathways in the sulfur cycle, including tracing the contribution of anthropogenic sulfate to groundwater (e.g., Van Donkelaar et al. 1995; Mitchell et al. 1998; Kaown et al. 2009). Typical δ<sup>34</sup>S values range from -15 to +14 ‰ for mineral sulfate, from -34 to +7 ‰ for sulfate from oxidation of reduced sulfur minerals, and from 0 to +6 ‰ for sulfate in atmospheric depositions in industrialized countries (Krouse and Mayer 2000; Rock and Mayer 2002; Mayer 2005).

Numerical models

The HYDRUS-1D software package uses several modeling concepts for evaluating solute transport (Šimůnek et al. 2008a, b). By combining HYDRUS-1D with PHREEQC (Parkhurst and Appelo 1999), HP1 (Jacques et al. 2008) is a significant expansion of HYDRUS-1D, while preserving most or all of the features and capabilities of the two original codes. The program can simulate precipitation/

dissolution, cation exchange, and sorption processes based on thermodynamic equilibrium, kinetics, or mixed equilibrium-kinetic reactions (Šimůnek et al. 2009). This model has been extensively used in simulating water and contaminant transport in variably saturated porous media (Jiang et al. 2010), and for a wide range of applications in both the research and management of irrigation systems with poor water quality (e.g., Gonçalves et al. 2006; Hanson et al. 2008; Forkutsa et al. 2009; Šimůnek et al. 2009).

HYDRUS-1D was applied in two ways in this work. First, to analyze field experimental data involving water contents and sulfates to lend greater credibility to simulations and allow for the extrapolation to different soil types, climatic conditions, and irrigation methods (using groundwater (1) in Table 1). Second, based on the above conclusions, to explain the impact of different flood irrigation water sources (local groundwater (2) and surface water from the Jinghe River in Table 1) on groundwater quality and the evolution of  $\text{SO}_4^{2-}$  in the future.

#### Water flow

Variably saturated water flow was simulated in HYDRUS-1D using the Richards equation, which requires input parameters describing the soil hydraulic properties. The van Genuchten–Mualem analytical model (van Genuchten 1980) was used to approximate the soil hydraulic properties. Details about the water flow module are given in the HYDRUS-1D technical manual (Šimůnek et al. 2008a, 2008b).

#### Solute transport

The partial differential equations governing one-dimensional advective-dispersive solute transport in a variably saturated rigid porous medium are defined in HYDRUS-1D as:

$$\frac{\partial \theta c_i}{\partial t} = \frac{\partial}{\partial x} \left( \theta D_i^w \frac{\partial c_i}{\partial x} \right) - \frac{\partial q c_i}{\partial x} - S c_{r,i} + R_i \quad (1)$$

where  $i$  ( $= 1, \dots, N_m$ ) is the aqueous species number ( $N_m$  is the total number of aqueous species),  $\theta$  is the volumetric soil water content [ $\text{L}^3 \text{L}^{-3}$ ],  $c_i$  is the aqueous concentration of the  $i$ th species [ $\text{ML}^{-3}$ ],  $q$  is the volumetric flux density [ $\text{L T}^{-1}$ ],  $S$  is the sink term in the water flow equation [ $\text{T}^{-1}$ ],  $c_r$  is the concentration of the sink term [ $\text{M L}^{-3}$ ],  $D^w$  is the dispersion coefficient in the liquid phase [ $\text{L}^2 \text{T}^{-1}$ ], and  $R_i$  is the general source/sink term representing geochemical reactions [ $\text{M L}^{-3} \text{T}^{-1}$ ]. This sink/source term contains heterogeneous equilibrium reactions, and homogeneous and heterogeneous kinetic reactions.

The parameter  $R_i$  in Eq. (1) represents equilibrium precipitation/dissolution reactions of minerals, and can be described as

$$\sum_{j=1}^{N_m} v_{ji}^p A_j^m = A_i^p \quad (2)$$

where  $i = 1, \dots, N_p$  ( $N_p$  is the number of minerals),  $A_j^m$  and  $A_i^p$  are the chemical formulae of the master and secondary species, respectively, and  $v_{ji}^p$  are the stoichiometric coefficients in the reaction. The superscript  $p$  refers to pure phases (minerals). For equilibrium conditions, the mass-action equation is

$$K_i^p = \prod_{j=1}^{N_m} (\gamma_j^m c_j^m)^{-v_{ji}^p} \quad (3)$$

where  $K_i^p$  is the equilibrium constant of a reaction (2), and  $\gamma_j^m$  is the activity coefficient of the  $j$  master species in the solution. The activity coefficients can be defined using the Davies equation or the extended Debye–Hückel equation (Langmuir 1997; Parkhurst and Appelo 1999). The activity of a pure phase (mineral) is assumed to be 1.

#### Initial conditions and input parameters

Initial water contents were specified according to TDR readings (Table 4) collected immediately before the start of the irrigation experiment on November 11, 2008 (an average value of the two TRIME probes; Fig. 1b). Solution compositions of waters used in the experiments and simulations are presented in Table 1.

The particle size distribution was obtained using the pipette method for particles with diameters smaller than 20  $\mu\text{m}$  (clay and silt fractions), and by sieving for particles between 200 and 2,000  $\mu\text{m}$  (coarse sand), and between 20 and 200  $\mu\text{m}$  (fine sand) (Table 4). The dry bulk density was measured using soil samples of known volume. Dispersivity ( $\lambda$ ) values were obtained using the HYDRUS-1D inverse model, based on  $\text{Cl}^{-1}$  concentrations during the irrigation experiment, and set to a uniform value throughout the soil profile. The sensitivity analysis of the impact of the  $\lambda$  value on  $\text{SO}_4^{2-}$  concentrations is presented in Table 5.

Table 6 lists the van Genuchten–Mualem parameters (van Genuchten 1980) for the soil hydraulic functions of particular soil layers. These were obtained using the Rosetta module (Schaap et al. 2001), which is implemented in the HYDRUS-1D software package, according to the particle size distribution and the bulk density of each layer of the soil.

According to the results of the mineralogical analysis (Liu et al. 2011), concentrations of reactive calcite ( $\text{CaCO}_3$ ) and dolomite  $\text{CaMg}(\text{CO}_3)_2$  were  $10^{-3}$  and  $10^{-4}$   $\text{mmol kg}^{-1}$ , respectively. Since no gypsum ( $\text{CaSO}_4 \cdot 2\text{H}_2\text{O}$ )

**Table 4** Selected physical and chemical soil characteristics of the soil profile before the irrigation experiment (2008/11/11)

	Depth (cm)					
	0–20	20–40	40–60	60–100	100–150	150–200
Coarse sand (%)	12.5	24.7	1.4	23.8	5.1	2.8
Fine sand (%)	37.1	32.2	46.3	46.2	56.8	58.3
Silt (%)	16.4	12.9	15.5	7.0	10.9	10.9
Clay (%)	34.0	30.0	36.8	23.0	27.2	28.0
Texture	Sandy clay loam					
Bulk density (g cm <sup>-3</sup> )	1.41	1.42	1.35	1.37	1.46	1.57
Water content (cm <sup>3</sup> cm <sup>-3</sup> )	0.18	0.20	0.20	0.22	0.23	0.27
Soil soluble ions						
pH (H <sub>2</sub> O)	8.7	8.2	8.4	8.9	8.4	8.5
Ca <sup>2+</sup> (mmol L <sup>-1</sup> )	0.96	0.78	0.58	0.51	0.43	0.49
Mg <sup>2+</sup> (mmol L <sup>-1</sup> )	0.58	0.62	0.47	0.47	0.52	0.51
Na <sup>+</sup> (mmol L <sup>-1</sup> )	0.10	0.27	0.91	0.96	1.30	1.20
K <sup>+</sup> (mmol L <sup>-1</sup> )	0.04	0.12	0.31	0.53	0.77	0.68
SO <sub>4</sub> <sup>2-</sup> (mmol L <sup>-1</sup> )	0.20	0.42	0.40	0.40	0.47	0.49
Cl <sup>-</sup> (mmol L <sup>-1</sup> )	0.62	0.40	0.25	0.37	0.62	0.67
Dispersivity (cm)	17.6	17.6	17.6	17.6	17.6	17.6

**Table 5** Changes in SO<sub>4</sub><sup>2-</sup> (%) at depths of 1 and 2 m based on the sensitivity analysis for selected model parameters

Depth (m)	K <sub>s</sub>		ρ		λ	
	+20 %	-20 %	+20 %	-20 %	+20 %	-20 %
1	3.1	1.3	1.2	1.1	2.4	2.5
2	3.3	1.6	1.1	1.3	3.0	3.3

K<sub>s</sub> saturated hydraulic conductivity, ρ bulk density, λ dispersivity

**Table 6** van Genuchten–Mualem parameters for the soil hydraulic functions

	Depth (cm)					
	0–20	20–40	40–60	60–100	100–150	150–200
θ <sub>r</sub> (cm <sup>3</sup> cm <sup>-3</sup> )	0.08	0.08	0.08	0.07	0.07	0.07
θ <sub>s</sub> (cm <sup>3</sup> cm <sup>-3</sup> )	0.43	0.44	0.45	0.41	0.41	0.41
α (cm <sup>-1</sup> )	0.02	0.021	0.02	0.024	0.023	0.023
n (-)	1.34	1.35	1.32	1.39	1.33	1.32
l (-)	0.5	0.5	0.5	0.5	0.5	0.5
K <sub>s</sub> (cm day <sup>-1</sup> )	19.0	27.9	19.0	33.4	22.2	21.5

θ<sub>r</sub> (cm<sup>3</sup> cm<sup>-3</sup>), residual soil water content; θ<sub>s</sub> (cm<sup>3</sup> cm<sup>-3</sup>), saturated soil water content; α (cm<sup>-1</sup>), parameter in the soil water retention function; n (-), parameter in the soil water retention function; l (-), tortuosity parameter in the conductivity function; K<sub>s</sub> (cm day<sup>-1</sup>), saturated hydraulic conductivity

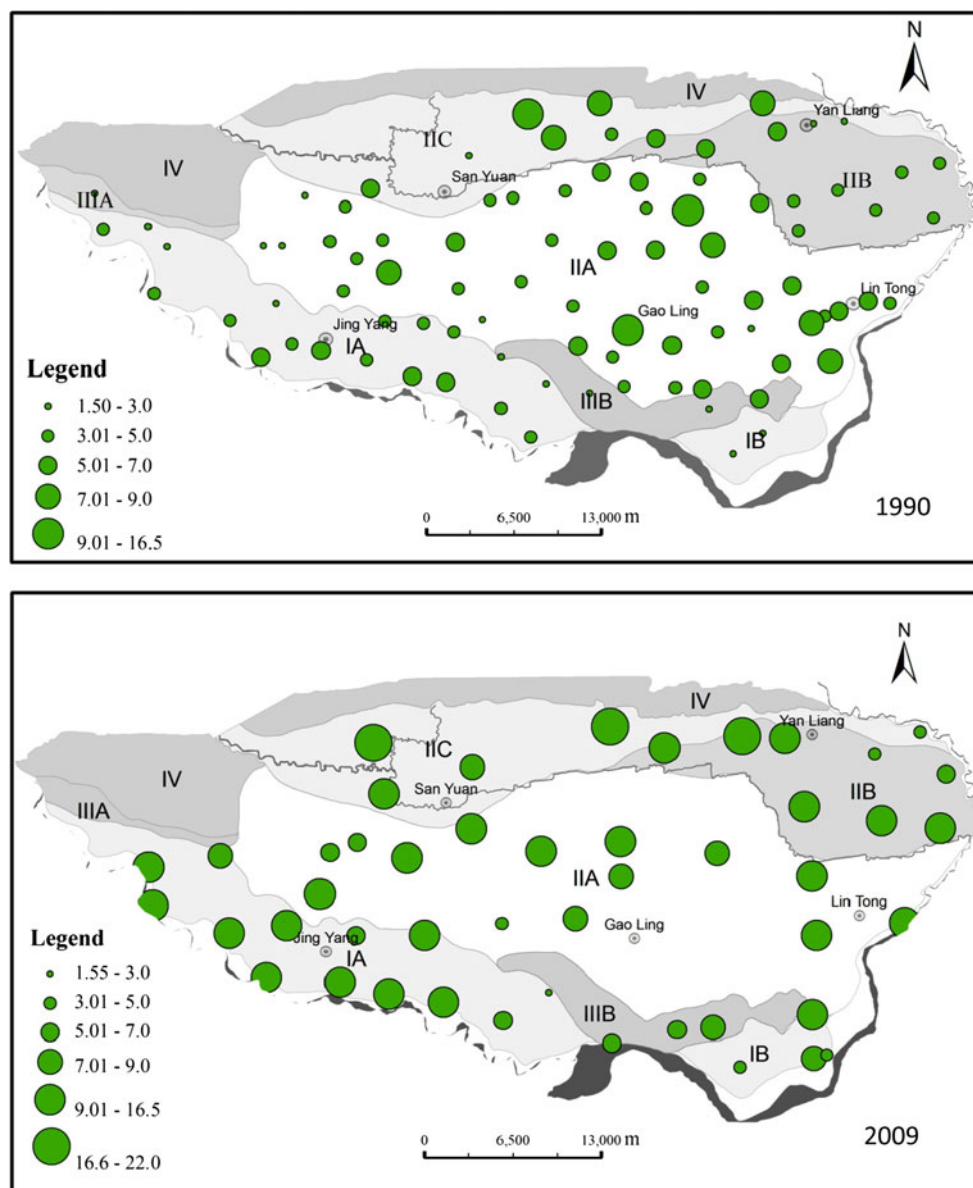
or mirabilite (Na<sub>2</sub>SO<sub>4</sub>·10H<sub>2</sub>O) were present, the initial values of reactive gypsum (CaSO<sub>4</sub>·2H<sub>2</sub>O) and mirabilite (Na<sub>2</sub>SO<sub>4</sub>·10H<sub>2</sub>O) in the soil were set to 0 mmol kg<sup>-1</sup>.

*Time-variable boundary conditions*

Atmospheric and free drainage conditions were used as boundary conditions at the surface and the bottom of the

soil profile, respectively. Atmospheric boundary conditions were specified using meteorological data collected at the Jinghuiuq meteorological station, and were used to compute daily values of the reference evapotranspiration rate (ET<sub>C</sub>) using the Penman–Monteith method (Allen et al. 1998). The reference evapotranspiration rate was assigned to potential evaporation, while potential transpiration was set to zero because the experimental sites were bare.

**Fig. 3** Distribution of groundwater  $\text{SO}_4^{2-}$  concentrations in the Jinghuiqu irrigation district in 1990 (*top*) and 2009 (*bottom*) ( $\text{mmol L}^{-1}$ )



## Results and discussion

### Sulfate geochemistry in groundwater

The  $\text{SO}_4^{2-}$  concentrations in groundwater samples obtained in April, 1990, November, 2008, and December, 2009 are summarized in Table 3. In 1990, the  $\text{SO}_4^{2-}$  concentrations in the groundwater of the entire irrigation area ranged from 1.5 to  $16.5 \text{ mmol L}^{-1}$ , with a mean value of  $4.8 \text{ mmol L}^{-1}$ . In 2008, the concentrations ranged from 2.0 to  $23.5 \text{ mmol L}^{-1}$ , with a mean value of  $9.23 \text{ mmol L}^{-1}$ , and in 2009 it ranged from 1.55 to  $22.0 \text{ mmol L}^{-1}$ , with a mean value of  $9.8 \text{ mmol L}^{-1}$  (Fig. 3). Although some wells analyzed in

1990 were not sampled in the following sampling periods, the percentage of the groundwater samples with elevated concentrations has been increasing within the entire irrigated area. Sulfate concentrations greater than  $600 \text{ mg L}^{-1}$  (about  $7 \text{ mmol L}^{-1}$ ) accounted for 16.5 % of the total irrigated area in 1990, while in 2009, they reached almost 85.1 %. The observed concentrations were far above the national drinking water standard of  $250 \text{ mg L}^{-1}$  (about  $3 \text{ mmol L}^{-1}$ ). Since elevated ion concentrations and distributions were similar in 2008 and 2009, only the 1990 and 2009 values are presented here.

While groundwater was characterized mainly as the  $\text{HCO}_3^-$  water type in 1990, in 2009,  $\text{SO}_4^{2-}$  was the

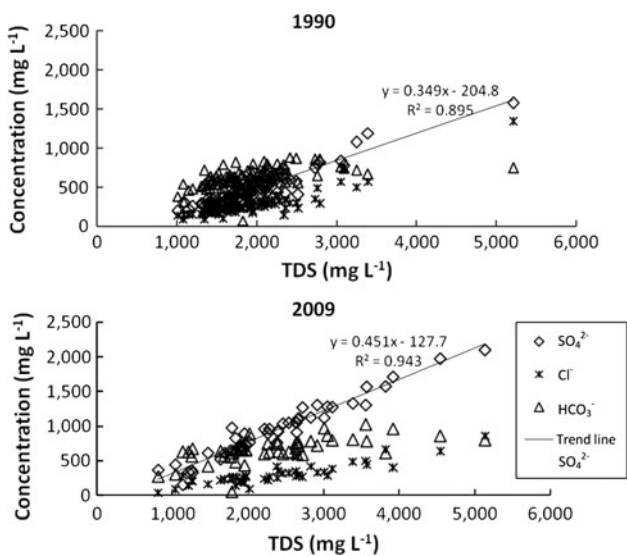


**Fig. 4** Relation between main anions ( $\text{SO}_4^{2-}$ ,  $\text{Cl}^-$ , and  $\text{HCO}_3^-$ ) and total dissolved solids (TDS) concentrations in groundwater in 1990 (top) and 2009 (bottom)

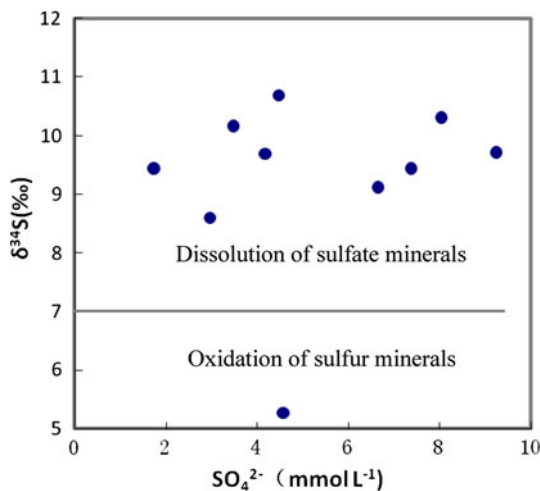


**Fig. 5** Relation between sulfate isotope ( $\delta^{34}\text{S}\text{-SO}_4$ ) and  $\text{SO}_4^{2-}$  concentrations in the irrigation district in 2008. The horizontal line at  $\delta^{34}\text{S} = 7 \text{ ‰}$  separates samples from two different  $\text{SO}_4^{2-}$  sources

dominant anion (Fig. 4). The extent of areas with elevated  $\text{SO}_4^{2-}$  increased as well. The source of evaluated  $\text{SO}_4^{2-}$  in groundwater will be identified first.

Characteristic  $\delta^{34}\text{S}$  values of sulfate

The sulfate concentrations of eleven groundwater samples varied from 1.75 to 9.24  $\text{mmol L}^{-1}$  and  $\delta^{34}\text{S}\text{-SO}_4^{2-}$  values ranged from +5.27 to +10.7 ‰ (Fig. 5). Although there is no baseline study on the level of natural  $\text{SO}_4^{2-}$  isotope values in groundwater in this area, the literature data (Ma and Fan 2005) and the relationship between  $\text{SO}_4^{2-}$

concentrations and  $\delta^{34}\text{S}\text{-SO}_4^{2-}$  indicate two different  $\text{SO}_4^{2-}$  sources (Fig. 5): oxidation of sulfur minerals and dissolution of sulfate minerals. Only  $\delta^{34}\text{S}\text{-SO}_4^{2-}$  of 5.27 ‰ for the D07 sample indicated oxidation of sulfur minerals.  $\delta^{34}\text{S}\text{-SO}_4^{2-}$  values for the other 10 groundwater samples ranged from 8.6 to 10.69 ‰, indicating dissolution from early sulfate minerals, such as gypsum and mirabilite, or from sulfate in the soil.

Transport simulations

Although the isotope analysis discussed above shows that  $\text{SO}_4^{2-}$  is mainly derived from the dissolution of sulfate in the soil, current mineralogical analysis did not detect any soluble sulfate minerals in the soil profile (Liu et al. 2011). To better understand this seeming anomaly, it is necessary to simulate the dissolution and leaching of sulfate using different irrigation water sources, and to evaluate its evolution based on current irrigation conditions in the Jinghuiqu irrigation district.

Volumetric water contents

The experiments started on November 11, 2008. Inputs for HYDRUS-1D consisted of the soil hydraulic parameters for the soil horizons (Table 4) and the quality of the applied irrigation water (groundwater (1) of Table 1). Measured and simulated water contents are presented in Fig. 6a (see also Liu et al. 2012). The figure shows that during the experimental period, water contents increased and then gradually decreased. Overall, simulated water contents closely mirrored measured values at all depths. The correlation coefficients (R) were equal to 0.93, 0.93, 0.9, and 0.81 at 1st, 2nd, 3rd, and 4th day after irrigation, respectively, with an overall correlation coefficient ( $R^2$ ) of 0.8 for the combined observations. This indicates a good agreement between measured and simulated values.

Sulfate ions

The input values of  $\text{SO}_4^{2-}$  concentrations for HP1 were obtained from samples collected before the start of the irrigation period and are presented in Table 4. The quality of the irrigation water (boundary concentrations), and  $\text{SO}_4^{2-}$  ion concentrations are presented in Table 1 [groundwater (1)]. Irrigating quantity was 18 cm, which is a common practice in the Jinghuiqu irrigation district.

Measured and simulated concentrations of  $\text{SO}_4^{2-}$  in six depths, 1 and 6 days after irrigation, are presented in Fig. 6b. The main differences were found at depths of 0–40 cm at 1 day. We believe that this disagreement could be largely explained by the sampling approach, as mixed samples were collected. Thus, the samples cannot

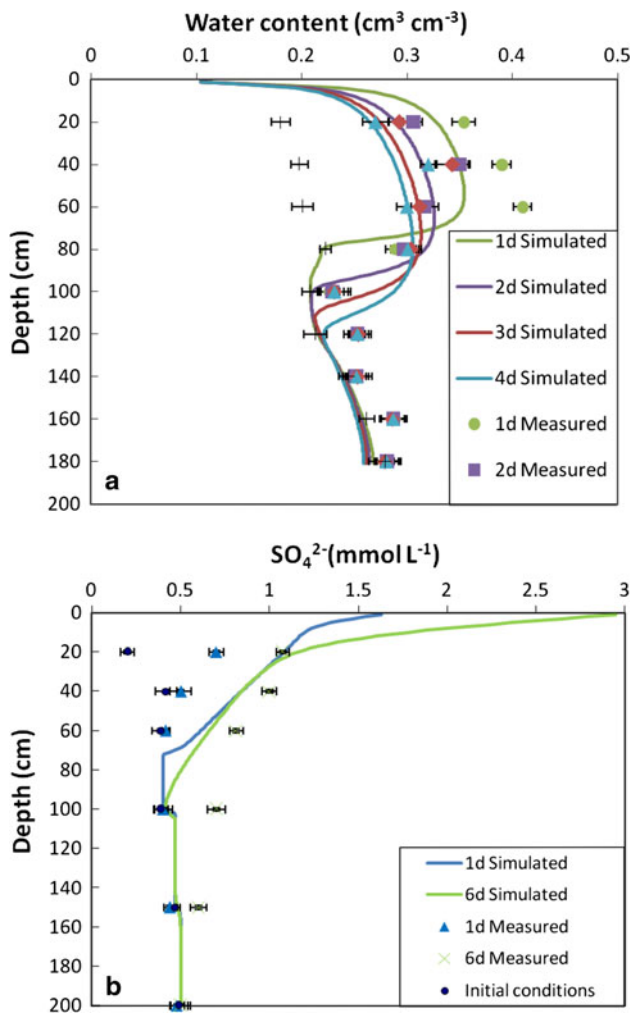


**Fig. 6** **a** Measured (TDR) and simulated (Hydrus) volumetric water contents (initial and 1, 2, 3, and 4 days after irrigation) and **b** measured and simulated (HP1)  $\text{SO}_4^{2-}$  concentrations (initial and 1 and 6 days after irrigation)

accurately represent point values, especially in the first day after flood irrigation, when water contents and solute concentrations changed quickly above the depth of 40 cm.

The simulations of the  $\text{SO}_4^{2-}$  concentrations resulted in a good agreement with measured values in the soil profile, with the correlation coefficients for  $\text{SO}_4^{2-}$  of 0.87 and 0.91 at days 1 and 6 after irrigation, respectively. This shows that the model can adequately simulate sulfate transport and dissolution in the soil profile.

#### Evaluation of different irrigation water sources

Based on this analysis of the simulation results of water contents and  $\text{SO}_4^{2-}$  concentrations after irrigation, it is necessary to use HP1 to further evaluate the impact of the flood irrigation method and different sources of irrigation water on groundwater quality under current irrigation practices.

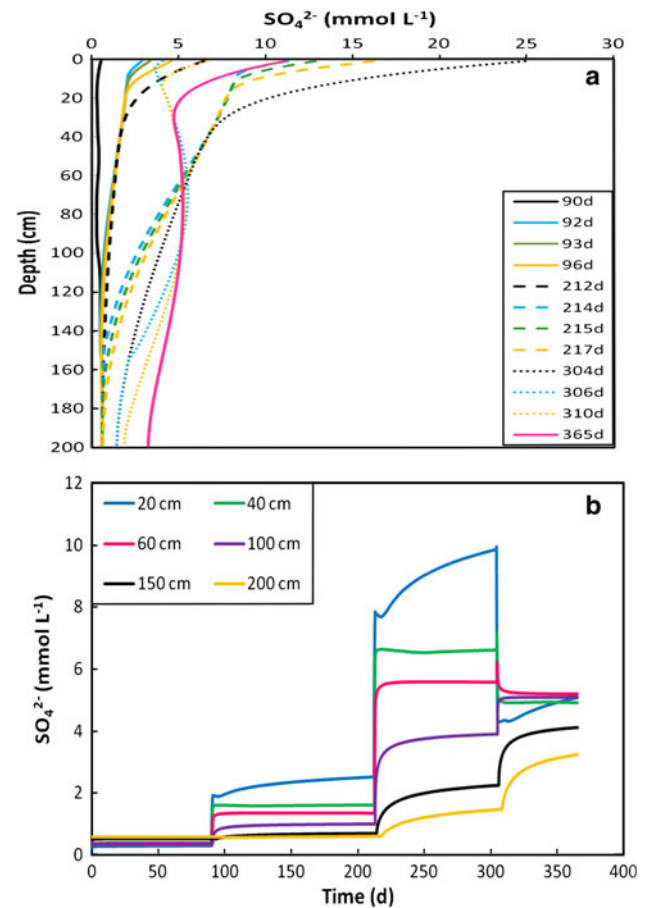


**Fig. 7** Simulated  $\text{SO}_4^{2-}$  concentrations at different times (days) **(a)** and depths (cm) **(b)**

To better explain involved processes, an evaluation period of 1 year was selected, with irrigations on April 1st (using surface water for winter wheat), August 1st (using groundwater for maize), and November 1st (using surface water for winter wheat), as commonly used in this area. The mean value of  $\text{SO}_4^{2-}$  was obtained in irrigation wells in 2009 [groundwater (2)] and in the Jinghe river water which were used as different irrigation sources (Table 1). Each time, the irrigation quantity was 18 cm. The same soil profile as in the field experiment described above was used. The soil conditions of that soil profile are presented in Table 4.

Simulated sulfate concentrations versus depth at different times are shown in Fig. 7a. Sulfate concentrations at days 90 (before irrigation), 92 (1 day after the first irrigation), 93 (2 days after the first irrigation), and 96 (5 days after the first irrigation) are displayed. Figure 7a shows that concentration values on day 92 were substantially higher than on day 90, primarily due to the mixing and leaching of the irrigation water (the sulfate concentrations of irrigation water were higher than the soil initial soluble concentrations). Between days 96 and 212 (before the second irrigation), sulfate concentrations increased in the soil profile at

depths above 30 cm due to evaporation of soil water. After the second irrigation, sulfate concentrations increased significantly on day 214 (1 day after the second irrigation) compared to day 212 (before irrigation). This is because we used groundwater with a high value of sulfate concentrations for irrigation. During this period, increased values of sulfate resulted largely from mixing of irrigation water. Between days 217 and 304 (before the third irrigation), sulfate concentrations increased at depths above 30 cm because of evaporation, and below 60 cm due to irrigation water moving downwards. The third irrigation (again using surface water) caused quite significant leaching of sulfates from the soil profile above 60 cm. Between days 306 and 310, and again at day 365, sulfate concentrations increased at depths above 30 cm due to evaporation, and at below 60 cm due to the downward movement of irrigation water.

During the simulation period, calculations showed that there was no dissolution and/or precipitation of gypsum and/or mirabilite. Calcite dissolved largely at depths above 20 cm, except when it briefly precipitated during the period when groundwater was used for irrigation (days of 215 and 217).

Simulated sulfate concentrations at depths of 20, 40, 60, 100, 150, and 200 cm of the soil profile are presented in Fig. 7b. The figure shows that each irrigation event had an impact on the increase of sulfate concentrations at all depths compared to the initial concentrations, especially when groundwater with elevated sulfate concentrations was used for irrigation (214–304 days). Soluble sulfate concentrations in the soil increased more when groundwater was used for irrigation than when surface water was used. After the third irrigation event (305 days), leaching occurred mainly in depths above 60 cm, where sulfate concentrations quickly decreased during the 2 days after irrigation. At deeper depths of 100 cm, sulfate concentrations were increasing during the entire simulated period. During the simulation, the sulfate concentration increased up to  $3.10 \text{ mmol L}^{-1}$  at a depth of 200 cm from the initial concentration of  $0.5 \text{ mmol L}^{-1}$ .

The transport of  $\text{SO}_4^{2-}$  in the upper part of the soil profile depends on the soil properties of the upper soil layers, which consist mainly of quaternary fluvial deposits (Fig. 2). To assess the effects of model parameters on the magnitude of  $\text{SO}_4^{2-}$  leaching, changes in  $\text{SO}_4^{2-}$  concentrations at depths of 1 and 2 m due to a 20 % change in the saturated hydraulic conductivity,  $K_s$ ; the dry bulk density,  $\rho$ ; and the longitudinal dispersivity,  $\lambda$  were calculated (Table 5). Table 5 shows that the effect of these selected parameters on  $\text{SO}_4^{2-}$  leaching is relatively minor.

Simulated results show that flood irrigation activities speed up the amount of sulfate leaching. They further indicate that irrigation water has been the main reason for elevated  $\text{SO}_4^{2-}$  concentrations in the groundwater since 1990, especially when water with elevated  $\text{SO}_4^{2-}$  concentrations

was used. Such water is not suitable as a source of water for irrigation, since it can speed up the progress of groundwater salinization. By contrast, the effects of rainfall can be neglected since it has minor effect on the solute movement.

## Conclusions

The  $\text{SO}_4^{2-}$  values in groundwater for the entire irrigation area increased from 1990 to 2009. The  $\delta^{34}\text{S}\text{-SO}_4^{2-}$  values indicated that the initial  $\text{SO}_4^{2-}$  concentrations resulted primarily from dissolution of sulfate minerals, but there was no additional dissolution of soluble sulfate minerals during the calculation period.

Comparing the sulfate and chloride concentrations in 1990, 2008, 2009, and 2011 (Table 3), ion concentrations increased when the amount of water decreased due to evaporation. However, mainly irrigation water had a great impact on the increase of sulfate concentrations in the shallow groundwater, especially when groundwater with elevated sulfate concentrations was used for irrigation. Changes in  $\text{SO}_4^{2-}$  concentrations presented in Fig. 3 and Table 3, as well as the results of the sensitivity analysis in Table 5, indicate that sources of irrigation water with elevated  $\text{SO}_4^{2-}$  concentrations have a significant impact on the evolution of groundwater  $\text{SO}_4^{2-}$  in the entire area. Measured  $\text{SO}_4^{2-}$  concentrations from 2009 and 2011 also reflect this increasing trend (Table 4).

Many wells in the Jinghuiqu area that are used as source of irrigation water have such high sulfate concentrations that their water can no longer be used for irrigation. During the last 20 years, elevated sulfate concentrations in the shallow groundwater are mainly due to the use of local groundwater for irrigation. Since groundwater has high levels of sulfate concentrations, it can significantly speed up groundwater salinization.

**Acknowledgments** This work was supported by the “Program on creation and intellectual importation for hydro-ecology and water security in the arid and semiarid regions” of the Ministry of Education and Foreign Expert Bureau of China (“111” project), and the project “Improving water use efficiency, and the experiment and demonstration of promoting new socialist countryside construction in the irrigation areas” of the Department of Water Resources of Shaanxi Province. Special thanks also go to the Jinghuiqu administration for data sharing.

## References

- Allen RG, Pereira LS, Raes D, Smith M (1998) Crop evapotranspiration—guidelines for computing crop water requirements. In: Irrigation and Drainage. Paper 56. FAO, Rome, Italy
- Bellier O, Mercier JL, Vergely P, Long C, Ning C (1988) Evolution sédimentaire et tectonique du graben cénozoïque de la Wei He (province du Shaanxi, Chine du Nord). Bull Soc Géol Fr IV(6):979–994

- Böhlke JK (2002) Groundwater recharge and agricultural contamination. *Hydrogeol J* 10:153–179
- Forkutsa I, Sommer R, Shirolova YL, Lamers JPA, Kienzler K, Tischbein B, Martius C, Vlek PLG (2009) Modeling irrigated cotton with shallow groundwater in the Aral Sea Basin of Uzbekistan: II. Soil salinity dynamics. *Irrig Sci* 27:319–330
- Gao C (2004) Test of the irrigation technique in the border field. *J Northwest Hydroelectr Power* 1:140–141 (in Chinese with English abstract)
- Gonçalves MC, Šimůnek J, Ramos TB, Martins JC, Neves MJ, Pires FP (2006) Multicomponent solute transport in soil lysimeters irrigated with waters of different quality. *Water Resour. Res.* 42. W08401. doi:10.1029/2005WR004802
- Groundwater Investigation Report of Jinghuiqu, Jinghuiqu Irrigation District (1983) Xi'an, Shaanxi Province, China, pp 112 (in Chinese with English abstract)
- Hanson BR, Šimůnek J, Hopmans JW (2008) Leaching with subsurface drip irrigation under saline, shallow ground water conditions. *Vadose Zone J* 7:810–818
- Jacques D, Šimůnek J, Mallants D, van Genuchten MT (2008) Modeling coupled hydrological and chemical processes: long-term uranium transport following mineral phosphorus fertilization. *Vadose Zone J* 7(2):698–711
- Jiang S, Pang LP, Buchan GD, Šimůnek J, Noonan MJ, Close ME (2010) Modeling water flow and bacterial transport in undisturbed lysimeters under irrigations of dairy shed effluent and water using HYDRUS-1D. *Water Res* 44:1050–1061
- Kaown D, Koh D-C, Mayer B, Lee K-K (2009) Identification of nitrate and sulfate sources in groundwater using dual stable isotope approaches for an agricultural area with different land use (Chuncheon, mid-eastern Korea). *Agric Ecosyst Environ* 132:223–231
- Krouse HR, Mayer B (2000) Sulfur and oxygen isotopes in sulfate. In: Cook PG, Herczeg AL (eds) *Environmental tracers in subsurface hydrology*. Kluwer Academic Press, Boston, pp 195–231
- Langmuir D (1997) *Aqueous environmental geochemistry*. Prentice Hall, New Jersey
- Li M (1998) Overview the Jinghuiqu irrigation system of expansion project construction management. *Shaanxi Water Resour* 2:30–31 (in Chinese with English abstract)
- Li Y, Ma X, Kang S (1999) Study on the optimal conjunctive use of surface and underground water in Jinghui irrigation region. *Trans Chin Soc Agric Eng* 1:130–134 (in Chinese with English abstract)
- Liu G (2002) Some sediment problem of the headwork project in Jinghuiqu. *Tech Seepage Cont* 2:37–42 (in Chinese with English abstract)
- Liu X (2005) Discussion on optimized arrangement of water resources in Jinghuiqu irrigation area of Shaanxi province. *J Water Resour Archit Eng* 3(2):62–64 (in Chinese with English abstract)
- Liu Y (2010) Dynamic variation characteristics and cause analysis of underground water level in Jinghui irrigation district. *Yangtze River* 8:100–107 (in Chinese with English abstract)
- Liu Y, Zhu H (2011) Characteristics of inferior variation of water environment and regulating capacity of groundwater reservoir in Jinghui Canal Irrigation District of China. *Trans Chin Soc Agric Eng* 6:19–23 (in Chinese with English abstract)
- Liu XH, Li L, Wang Z (2011) Biogeochemistry characteristics of nitrogen in unsaturated soils of JingHuiQu irrigation district, China. In: ISWREP 2011, proceedings of international symposium on water resource and environmental protection, vol 2, pp 959–962
- Liu XH, Sun SJ, Ji P, Šimůnek J (2012) Identification of nitrate sources in groundwater and modeling of nitrate transport after flood irrigation using HYDRUS-1D. *Hydrol Sci J* (in press)
- Ma ZY, Fan JJ (2005). Sulfate forming from groundwater in western Weibei karst area, Shaanxi Province. *Coal Geol Explor* 33(3):45–48 (in Chinese with English abstract)
- Mayer B (2005) Assessing sources and transformations of sulfate and nitrate in the hydrosphere using isotopic techniques. In: Aggarwal PK, Gat JR, Froehlich FO (eds) *Isotopes in the water cycle: past, present, and future of a developing sciences*. IEA, Netherlands, pp 67–89
- Mitchell MJ, Krouse HR, Mayer B, Stam AC, Zhang Y (1998) Use of stable isotopes in evaluating sulfur biogeochemistry of forest ecosystems. In: Kendall C, McDonnell JJ (eds) *Isotope tracers in catchment hydrology*. Elsevier, Amsterdam
- Parkhurst DL, Appelo CAJ (1999) *User's guide to PHREEQC (Version 2)—a computer program for speciation, batch-reaction, one-dimensional transport, and inverse geochemical calculations*. Water-resources investigations, report 99–4259. Denver, Co., USA, p 312
- Ramos TB, Šimůnek J, Gonçalves MC, Martins JC, Prazeres A, Castanheira NL, Pereira LS (2011) Field evaluation of a multicomponent solute transport model in soils irrigated with saline waters. *J Hydrol* 407(1–4):129–144
- Rock L, Mayer B (2002) Isotopic assessment of sources and processes affecting sulfate and nitrate in surface water and groundwater of Luxembourg. *Isotopes Environ Health Stud* 38(4):191–206
- Rock L, Mayer B (2009) Identifying the influence of geology, land use, and anthropogenic activities on riverine sulfate on a watershed scale by combining hydrometric, chemical and isotopic approaches. *Chem Geol* 262:121–130
- Schaap MG, Leij FJ, van Genuchten MT (2001) Rosetta: a computer program for estimating soil hydraulic parameters with hierarchical pedotransfer functions. *J Hydrol* 251:163–176
- Shanley JB, Mayer B, Mitchell MJ, Michel RL, Bailey SW, Kendall C (2005) Tracing sources of stream water sulfate during snowmelt using S and O isotope ratios of sulfate and  $^{35}\text{S}$  activity. *Biogeochemistry* 76:161–185
- Šimůnek J, Šejna M, Saito H, Sakai M, van Genuchten MT (2008) The HYDRUS-1D software package for simulating the movement of water, heat, and multiple solutes in variably-saturated media. Version 4.0 HYDRUS Software Series 3, Department of Environmental Sciences, University of California Riverside, Riverside, CA, USA, pp 315
- Šimůnek J, van Genuchten MT, Šejna M (2008b) Development and applications of the HYDRUS and STANMOD software packages, and related codes. *Vadose Zone J* 7(2):587–600
- Šimůnek J, Jacques D, Twarakavi NKC, van Genuchten MT (2009) Modeling subsurface flow and contaminant transport as influenced by biological processes at various scales using selected HYDRUS modules. *Biologia* 64(3):465–469. doi:10.2478/s11756-009-0106-7
- Szynkiewicz A, Witcher JC, Modelska M, David MB, Lisa MP (2011) Anthropogenic sulfate loads in the Rio Grande, New Mexico (USA). *Chem Geol* 283:194–209
- Van Donkelaar C, Hutcheon IE, Krouse HR (1995)  $\delta^{34}\text{S}$ ,  $\delta^{18}\text{O}$ ,  $\delta\text{D}$  in shallow groundwater: tracing anthropogenic sulfate and accompanying groundwater/rock interactions. *Water Air Soil Pollut* 79:279–298
- van Genuchten MT (1980) A closed form equation for prediction the hydraulic conductivity of unsaturated soils. *Soil Sci Soc Am J* 44:892–898
- West LJ, Truss SW (2006) Borehole time domain reflectometry in layered sandstone: impact of measurement technique on vadose zone process identification. *J Hydrol* 319:143–162
- Zhao A, Fei LJ (2006) Molding the conjunctive use of surface water and groundwater in irrigation area—take Jinghuiqu for an example. *J Northwest Hydroelectr Power* 22(5):23–27 (in Chinese with English abstract)